

## 3D problems of rotating detonation wave in a ramjet engine modeled on a super-computer

V.F. Nikitin<sup>1,2</sup>, Yu.G. Filippov<sup>1</sup>, L.I. Stamov<sup>1,2</sup>, E.V. Mikhachenko<sup>1,2</sup>

<sup>1</sup> Lomonosov Moscow State University, <sup>2</sup> SRISA RAS

A rotating detonation engine (RDE) combustion chamber was modeled in the work numerically using 3D geometry. The RDE is a new type of engines capable to create higher thrust than the traditional ones, which are based on the combustible mixture deflagration process. In the numerical experiment, different scenarios of the engine performance were obtained. The calculations were made at a compact super-computer APK-5 with a peak performance of 5.5 Tera Flops.

Keywords: Mathematical Modeling, Detonation, Deflagration, RDE, Ramjet.

### 1 Introduction

The optimization of modern engines based on the traditional design is now close to its technological limit. The engines performance may be increased only with the use of radically new technical solutions [1]. One of those solutions is the development of detonation engines; we deal with an engine with a rotating detonation [2]. The numerical modeling of the processes in a combustion chamber is an important stage in the investigation of its design and further usage. The mathematical model includes equations for multicomponent gas mixture, it considers chemical reactions and turbulent transport of mass, momentum and energy. In order to resolve such events as detonation cells development and thin wave configurations, one should have a rather thin computational mesh, and it contributes to the complexity. Therefore, the problem should be solved using big computational resources, high precision approximation schemes, and effective parallelization methods: OpenMP, MPI, CUDA, etc. In order to solve such problems, the authors have created a parallel code with the AUSM [3], the MUSCL [4] methods incorporated. The current research uses the OpenMP version of the computer program.

### 2 Mathematical model

The mathematical model contains the governing equations (differential and algebraic), boundary and initial conditions. The details of the numerical realization together with the computational mesh design and the placement of variables on the mesh, is a subject of the numerical model.

#### 2.1 The balance equations

To model a multicomponent gas mixture, we use the following system of balance equations:

$$\frac{\partial \rho_k}{\partial t} + \frac{\partial}{\partial x_j} (\rho_k u_j) - \frac{\partial J_{k,j}}{\partial x_j} = \mathcal{G}_k \quad (2.1)$$

$$\frac{\partial \rho u_i}{\partial t} + \frac{\partial}{\partial x_j} (\rho u_i u_j) + \frac{\partial p}{\partial x_i} - \frac{\partial \tau_{i,j}}{\partial x_j} = 0 \quad (2.2)$$

$$\frac{\partial E_T}{\partial t} + \frac{\partial}{\partial x_j} ((E_T + p) u_j) - \frac{\partial}{\partial x_j} (J_{T,j} + u_i \tau_{i,j}) = \mathcal{Q} \quad (2.3)$$

Here  $\rho_k$  is partial density of a species  $k$ ,  $J_{k,j}$  are vector components of the species  $k$  diffusion flux,  $\mathcal{G}_k$  is the intensity of the species  $k$  origination in chemical reactions,  $\rho$  is the gas mixture density,  $u_j$  are vector components of gas velocity,  $p$  is the mixture pressure,  $\tau_{i,j}$  are the tensor components of viscous and turbulent stresses,  $E_T$  is total energy of the gas volume unit consisting of thermal, chemical, kinetic

and turbulent energy,  $\mathbf{J}_{T,j}$  are vector components of the energy diffusion flux,  $\mathcal{Q}$  is the heat flux from an external source.

## 2.2 Additional algebraic relations

$$\rho = \sum_{k=1}^{N_c} \rho_k, Y_k = \frac{\rho_k}{\rho}, X_k = \frac{\rho_k}{W_k} \quad (2.4)$$

Here:  $Y_k$  is the mass share of the species  $k$ ,  $X_k$  is the molar density (in terms of many works on chemical kinetics it is named a molar concentration),  $W_k$  is the molar mass of a species. The pressure  $p$  is defined as the spherical part of the stresses tensor (with the opposite sign), and it is a sum of thermal pressure  $p_0$  of perfect gases mixture, and an additive corresponding to turbulent pulsations, which is modeled by means of the turbulent energy per mass unit  $K$ :

$$p = p_0 + \frac{2}{3}\rho K, p_0 = R_G T \sum_{k=1}^{N_c} X_k \cdot \quad (2.5)$$

The total energy of a volume unit is the following sum:

$$E_T = E + \rho \frac{u^2}{2} + \rho K, u^2 = u_j u_j \cdot \quad (2.6)$$

The total energy  $E_T$  is therefore the sum of internal (thermal and chemical) energy, kinetic, and turbulent energy. The internal energy of a volume unit is modeled as follows:

$$E = \sum_{k=1}^{N_c} X_k E_k(T) = R_G T \sum_{k=1}^{N_c} X_k \cdot (\hat{H}_k(T) - 1) \cdot \quad (2.7)$$

Here,  $E_k$  is an internal energy of a species mole,  $\hat{H}_k(T)$  is dimensionless enthalpy of a species containing the formation enthalpy at a reference temperature  $T_{ref}$  (chemical energy). Those functions are the basis of the species thermodynamic description; for many species, they are either tabulated, or approximated with polynomials. In the current research, they are taken from [4]; their format (two-interval) is described in [3] and [5]. We joined those temperature intervals into a single, and obtained the polynomial coefficients using the linear regression analysis based on the least squares technique.

## 2.3 Chemical kinetics

In the current research, the chemical sources  $\mathcal{Q}_k$  depend on temperature  $T$  and the set of molar densities  $\mathbf{X} = \{X_k\}$ ; the sum of those sources is zero due to the law of mass conservation in chemical reactions:

$$\mathcal{Q}_k = W_k \hat{\omega}_k(T, \mathbf{X}), \sum_{k=1}^{N_c} \mathcal{Q}_k = 0 \cdot \quad (2.8)$$

Here  $\hat{\omega}_k$  is the intensity of a species mole origination in a volume unit.

Some more strict laws for chemical interactions exist, e.g. the conservation of mass for each element. Those laws are considered in the chemical mechanism, and sometimes can reduce the computations and increase the precision. A general form for the chemical sources is usually complex, and it consists of many nonlinear terms; a typical expression is as follows:

$$\hat{\omega}_k = \sum_r \nu_{r,k} \omega_r, \omega_r = M_r(\mathbf{X}) \left[ k_{F,r}(M_r, T) \prod_j X_j^{\alpha_{r,j}} - k_{R,r}(M_r, T) \prod_j X_j^{\beta_{r,j}} \right] \quad (2.9)$$

Here,  $\omega_r$  is the reaction  $r$  speed (intensity),  $\nu_{r,k}$  is an algebraic stoichiometric coefficient for a species  $k$  in the reaction  $r$ , this coefficient is positive for the species being produced, and negative for those being consumed.  $M_r$  is the influence coefficient of non-changing components, which is equal to unity in the lack of such an influence,  $k_{F,r}$  is the direct reaction speed coefficient; it usually depend on tempera-

ture only, but for some “falloff” reactions it depends on  $M_r$ ,  $k_{B,r}$  is the reverse reaction speed,  $\alpha_{r,k}$  are degrees for species in a direct reaction (usually but not always they are non-zero for the input species),  $\beta_{r,k}$  are the degrees for the reverse reactions.

In case of elementary reactions, the degrees for species in the expression (2.9) are the same with the input and output stoichiometric coefficients. The reverse reaction speed coefficients were calculated to provide the dynamical reach of chemical equilibrium in the case of zero fluxes and constant density and internal energy:

$$k_{B,r} = k_{F,r} \exp\left(\sum_{k=1}^{N_c} \nu_{r,k} \left(\hat{H}_k(T) - \hat{S}_k(T) - 1\right)\right) \left(\frac{R_g T}{P_{ref}}\right)^{\sum_{k=1}^{N_c} \nu_{r,k}}. \quad (2.10)$$

For each direct reaction, its coefficient is modeled with an Arrhenius formula.

## 2.4 Turbulence model and transport

The current research uses the Wilcox k- $\omega$  model [2]:

$$\frac{\partial \rho K}{\partial t} + \frac{\partial}{\partial x_j} (\rho K u_j) - \frac{\partial}{\partial x_j} \left( (\mu + \sigma^* \mu_T) \frac{\partial K}{\partial x_j} \right) = \tau_{i,j}^T \frac{\partial u_i}{\partial x_j} - \beta^* \rho K \omega, \quad (2.11)$$

$$\frac{\partial \rho \omega}{\partial t} + \frac{\partial}{\partial x_j} (\rho \omega u_j) - \frac{\partial}{\partial x_j} \left( (\mu + \sigma \mu_T) \frac{\partial \omega}{\partial x_j} \right) = \alpha \frac{\omega}{K} \tau_{i,j}^T \frac{\partial u_i}{\partial x_j} - \beta \rho \omega^2. \quad (2.12)$$

$$\mu_T = \rho \frac{K}{\omega} \quad (2.13)$$

Here  $K$  is the kinetic energy of pulsations per mass unit,  $\mu$  is the molecular viscosity of the gas mixture,  $\mu_T$  is the turbulent (eddy) viscosity,  $\tau_{i,j}^T$  is the turbulent part of the stresses tensor,  $\omega$  is the intensity of the turbulent energy decay (dissipation) far away from walls and in lack of the turbulent energy input sources,  $\alpha=5/9$ ,  $\sigma=\sigma^*=1/2$ ,  $\beta=3/40$ ,  $\beta^*=9/100$  are constant parameters of the Wilcox model.

The turbulent part of the stresses tensor deviator is:

$$\tau_{i,j}^T = \rho \frac{K}{\omega} \left( \frac{\partial u_i}{\partial x_j} + \frac{\partial u_j}{\partial x_i} - \frac{2}{3} \frac{\partial u_s}{\partial x_s} \delta_{i,j} \right). \quad (2.14)$$

The molecular viscosity of the gas mixture is calculated using the species viscosity and molar densities as:

$$\mu = \frac{\sum_{k=1}^{N_c} X_k \mu_k(T)}{\sum_{j=1}^{N_c} X_j \phi_{k,j}(T)}. \quad (2.15)$$

The effective mixture viscosity is lower than the weighted average due to the binary influence coefficients  $\phi_{k,j}$ . A simple method to compute them was published in [6]:

$$\phi_{k,j} = \frac{1}{\sqrt{8}} \left( 1 + \frac{W_k}{W_j} \right)^{\frac{1}{2}} \left( 1 + \left( \frac{\mu_k}{\mu_j} \right)^{\frac{1}{2}} \left( \frac{W_j}{W_k} \right)^{\frac{1}{4}} \right)^2. \quad (2.16)$$

A molecular viscosity is calculated using physical molecular constants taken from the database [7], and the method of computation was taken from [6].

To calculate the fluxes of mass and energy  $J_{k,j}$  and  $J_{T,j}$ , and the stresses tensor deviator  $\tau_{i,j}$ , we used a model taking into account the turbulent transport calculated by means of the Wilcox model [2]. In most cases, the turbulent transport supersedes the molecular, and the last is made using simplified technique: constant Prandtl  $Pr$  and Schmidt  $Sc$  numbers hypothesis:

$$\begin{aligned}
 J_{k,j} &= \left( \frac{\mu}{Sc} + \frac{\mu_T}{Sc_T} \right) \frac{\partial Y_k}{\partial x_j}, \\
 J_{T,j} &= \left( \frac{\mu}{Pr} + \frac{\mu_T}{Pr_T} \right) \frac{\partial h}{\partial x_j} + (\mu + \mu_T) \frac{\partial K}{\partial x_j}, \\
 \tau_{i,j} &= (\mu + \mu_T) \left( \frac{\partial u_i}{\partial x_j} + \frac{\partial u_j}{\partial x_i} - \frac{2}{3} \frac{\partial u_s}{\partial x_s} \delta_{i,j} \right).
 \end{aligned}
 \tag{2.17}$$

Here,  $Sc_T$ ,  $Pr_T$  are constant turbulent Schmidt and Prandtl numbers,  $h=H/\rho$  is the enthalpy per mass unit,  $\delta_{ij}$  is the Kronecker symbol. The volume unit enthalpy is computed as follows:

$$H = R_G T \sum_{k=1}^{N_c} X_k \hat{H}_k(T).
 \tag{2.18}$$

## 2.5 The species list and the kinetic mechanism

Hydrogen, oxygen and nitrogen were the initial and the inflow mixture components. In the process of combustion, besides the main product, water vapor, numerous products (radicals) are originated; at high temperature they still persist in the mixture, and at lower temperature they decay. We used the following set of species:  $\{H_2O, OH, H, O, HO_2, H_2O_2, O_2, H_2, N_2\}$ . The research used a kinetic mechanism described in the Maas & Pope work [9] (1992). The mechanism consisted of 20 reversible reactions.

## 3 Results

A model combustion chamber of a ramjet detonation engine was treated as a test. Geometrically, it is a hollow cylinder with the cylindrical internal body, which ends up as a cone. The fuel flow into the chamber through numerous injectors (premixed rich composition  $[H_2]: [O_2]=3:1$ , stagnant pressure 10 bar, stagnant temperature 258 K, Mach number at each orifice 1). At the initial instance, the chamber is filled with air at 1 bar pressure and 300 K temperature. The ignition is made by means of an external energy source into a small spherical portion:  $r_{ign}=2.5$  mm during the first  $t_{ign}=10^{-6}$  seconds from the initial instance, and with power per volume as high as  $Q=20$  kW/mm<sup>3</sup>.

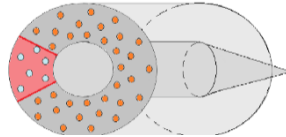


**Fig. 1.** The combustion chamber geometry.

The work area length was  $L=10$  cm, the maximal radius of the work area  $R = 2.5$  cm, the inner body radius  $R_b = 1.5$  cm, the inner body length without the terminating cone was  $L_b=3$  cm, the terminating cone length  $L_c=3$  cm, the number of injectors  $N_f=72$ , their orifices radii were  $r = 0.2$  cm. The test problem was solved on a structured cubic cells mesh made of  $\approx 1.3 \cdot 10^6$  cells; the size of a cell was 0.5 mm.

The Fig. 2 shows pressure in the ramjet engine combustion chamber for different times shown in a cross section OYZ at the distance of 0.5 cm from the injectors end. The Fig. 3 shows temperature in this cross section. The Figs. 4 and 5 show 3D distribution of pressure and temperature, respectively, at a given time.

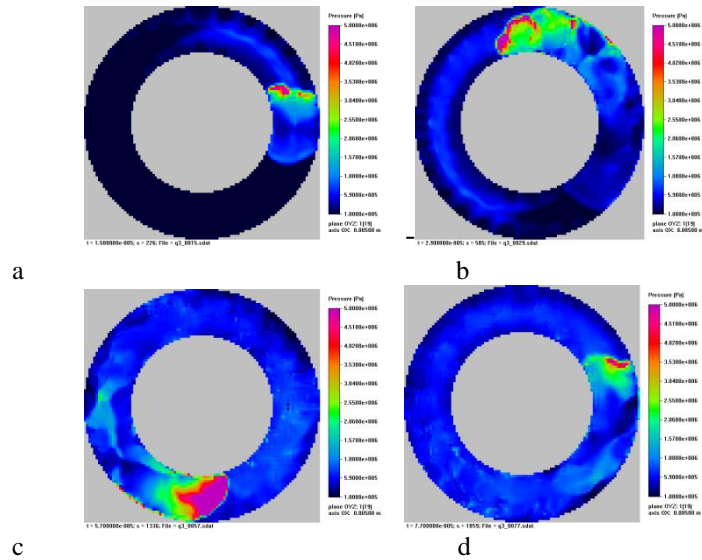


**Fig. 2.** Pressure in the cross section: a)  $t=1.5\mu\text{s}$ , b)  $t=2.9\mu\text{s}$ , c)  $t=5.7\mu\text{s}$ , d)  $t=7.7\mu\text{s}$ .

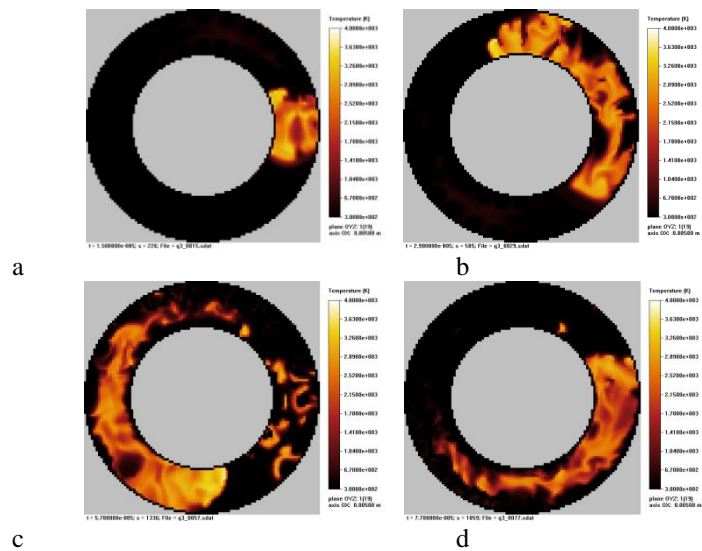


**Fig. 3.** Temperature in the cross section: a)  $t=1.5\mu\text{s}$ , b)  $t=2.9\mu\text{s}$ , c)  $t=5.7\mu\text{s}$ , d)  $t=7.7\mu\text{s}$

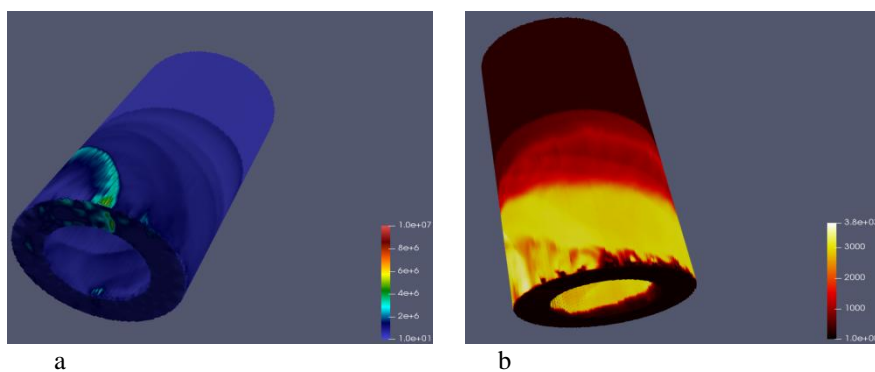


**Fig. 4.** 3D pressure (a) and temperature (b) distribution at  $t=5.7\mu\text{s}$ .

As the result of the numerical experiment, for the given parameter set, we obtained a galloping detonation wave rotating around the bottom of the combustion chamber. In the beginning, a stable detonation wave originates, but after  $70\mu\text{s}$  it splits into two, even 3 waves, which then join into a sin-

gle detonation wave. After that, in some time the process repeats: lateral waves reflections from walls contribute to it.

### 3.1 The calculating system

The calculations were performed at a computational system with two INTEL Xeon E5-2650 processors with 8 computational cores and 16 threads in each, and on a computational node of a native super computer APK-5. [22] The Fig. 6 shows the results of a computational test on both: acceleration due to the number of OpenMP threads, against a single thread. The time stepping algorithm was organized into 4 main cycles by cells and faces; the last cycle assembling all the fluxes together and creating the new state of parameters. The promotion to the 2<sup>nd</sup> order approximation in time was made repeating this algorithm once more with some modifications; the details are shown in [21].

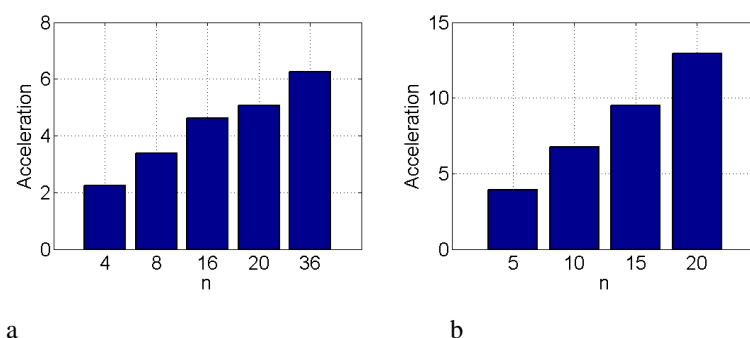


Fig. 5. Acceleration for the server node (a) and for the APK-5 (b).

## 4 Conclusions

The problem is computationally complex. The modeled configuration included more than 9 million of cells. We obtained more than 6 times acceleration on the server system, and more than 12 times acceleration on the computer APK-5. The APK-5 node acceleration is better due to high frequency of processors and its new architecture in comparison with the processors of the another server node. In order to calculate the bigger devices, and/or to use better mesh refinement to resolve more details of the process, one should use all the computational nodes. To do this, it is worth to add the MPI parallelization paradigm into the computational algorithm.

The work was made with the support of the RFBR grant № 18-07-00889.

## References

1. Bulat P. V., Volkov K. N. Detonation jet engine. part 2 – construction features // International Journal of Environmental and Science Education (IJESE). — 2016. — Vol. 11, no. 12. — P. 5020–5033.
2. G. Roy, S. Frolov, Eds. Deflagrative and Detonative Combustion. Moscow: Torus Press, 2010, 520p. ISBN 978-5-94588-071-9.
3. Hirsch, C. (1990), Numerical Computation of Internal and External Flows, vol 2, Wiley.
4. Liou, M.-S., “A Sequel to AUSM: AUSM+” J. Comput. Phys., Vol. 129, 364-382, 1996.
5. N.N. Smirnov, V.F. Nikitin, Sh. Aliari – Shurekhdeli. Transitional modes of waves propagation in metastable systems. Physics of combustion and explosion, 44, 5 (2008), c. 25-37 (in Russian).
6. D.C. Wilcox. Turbulence modeling for CFD. DCW Industries, Inc. La Canada, 1993.
7. CHEMKIN. A software package for the analysis of gas-phase chemical and plasma kinetics. CHE-036-1. Chemkin collection release 3.6. Reaction Design, September 2000.
8. Marinov, N.M., Pitz, W.J., Westbrook, C.K., Hori, M., and Matsunaga, N. An Experimental and Kinetic Calculation of the Promotion Effect of Hydrocarbons on the NO-NO<sub>2</sub> Conversion in a Flow Reactor. Proceedings of the Combustion Institute, Volume 27, pp. 389-396, 1998. (UCRL-JC-129372). UCRL-WEB-204236.

9. R.J. Kee, J.A. Miller, and T.H. Jefferson. Chemkin: a general-purpose, problem-independent, transportable Fortran chemical kinetics code package. Sandia National Laboratories Report SAND80-8003 (1980).
10. Transport. A software package for the evaluation of gas-phase, multicomponent transport properties. TRA-036-1, CHEMKIN collection, release 2000
11. Connaire, M. O., Curran, H J., Simmie, J. M., Pitz, W. J. and Westbrook, C.K., "A Comprehensive Modeling Study of Hydrogen Oxidation", International Journal of Chemical Kinetics, 36:603-622, 2004: UCRL-JC-152569.
12. Combustion onset in non-uniform dispersed mixtures / N. N. Smirnov, V. F. Nikitin, V. R. Dushin et al. // Acta Astronautica. — 2015. — Vol. 115. — P. 94–101.
13. Frolov S.M., Dubrovskii A.V., and Ivanov V. S. Three-dimensional numerical simulation of the operation of the rotating detonation chamber. Russian Journal of Physical Chemistry B, 2012, Vol. 6, No. 2, pp. 276-288
14. Wolanski P. Detonative propulsion // Proceedings of the Combustion Institute. 2013. Vol. 34. No. 1. P. 125-158
15. Wolanski, P., Kindracki, J., Fujiwara, T., Oka, Y., and Shima-uchi, K., (2005). An Experimental Study of Rotating Detonation Engine, 20th International Colloquium on the Dynamics of Explosions and Reactive Systems<sup>[1]</sup>, 31 July - 5 August, 2005, Montreal, Canada
16. U. Maas, and S.B. Pope. Simplifying chemical kinetics: intrinsic low-dimensional manifolds in composition space. Combustion and Flame, 88, 239-264 (1992).
17. Fletcher K. Computational techniques for fluid dynamics. Vol. 1 and 2. Second edition. Springer – Verlag, 2006.
18. N.N. Smirnov, V.F. Nikitin, Yu.G. Phylippov. Deflagration to detonation transition in gases in tubes with cavities. Journal of Engineering Physics and Thermophysics, 83, 6 (2010), pp. 1287-1316
19. Rybakin B. P., Stamov L. I., Egorova E. V. Accelerated solution of problems of combustion gas dynamics on gpus // Computers and Fluids. — 2014. — Vol. 90. — P. 164–171.
20. Detonation onset following shock wave focusing / N. N. Smirnov, O. G. Penyazkov, K. L. Sevrouk et al. // Acta Astronautica. — 2017. — Vol. 135. — P. 114–130.
21. Numerical investigations of hybrid rocket engines / V. B. Betelin, A. G. Kushnirenko, N. N. Smirnov et al. // Acta Astronautica. — 2018. — Vol. 144. — P. 363–370.
22. APK-5 documentation. URL: <http://compcenter.org/super-evm-apk-5>.